

Satellite Differential Code Bias Estimated Using EGYNET: A Local Egyptian Permanent Network



Mohammed A. Abid^{1*}, Ashraf Mousa²

¹ Faculty of Engineering, Tikrit University, Tikrit 34001, Iraq

² National Research Institute of Astronomy and Geophysics, Helwan 11928, Egypt

Corresponding Author Email: moh1963@tu.edu.iq

<https://doi.org/10.18280/i2m.190606>

ABSTRACT

Received: 12 August 2020

Accepted: 23 November 2020

Keywords:

satellite differential code bias, gobble positioning system, Global Navigation Satellite System

This paper proposes to determine the GPS satellites DCB using nine GPS receivers located in the middle of Egypt. During four seasons and 36 days characterized by quiet geomagnetism, the performance of the proposed method is examined. The dual GPS data selected is used and applied to the GPS receiver chain notes. The Bernese program V.5 is used to estimate DCBs from the data of a single GPS station where the results of the algorithm operation are compared to the CODE DCB data and the main differences in GLONASS data are recorded. According to the comparison of the results between the proposed method and the currently existing methods, it can be shown that the accuracy of the DCB estimates is at a level of about 0.31 and 0.17 ns.

1. INTRODUCTION

GPS primarily uses signals from group of satellites to determine the location and speed of a fixtures or mobile object over or nearby the earth's surface. Many satellites relay more than two L-band carrier electromagnetic waves, i.e. L1, L2, L2C, and L5, simultaneously. However, absolute simultaneity is not feasible, meaning that there is a time gap between the signal transmissions. It is known as satellite inter-frequency bias (IFB) and each satellite has a particular IFB [1]. For only a few GPS receivers it is possible to determine the differential instrumental bias by internal calibration. For the satellites, a prelaunch calibration is made, but it shows poor agreement with the values estimated using later observations [1].

The characteristics of the hardware delay depend primarily on the output of the corresponding instruments and their values for each sighting and frequency are different. Furthermore, the DCB is a general context in which the hardware biases of a given experiment can be implemented as a norm, and categorized in two categories: the bias between the inter-frequency observations, which reflects the bias of the observations at the two distinct frequencies; and the bias between the two observations at the same frequency [2].

Due to the combined satellite and receiver biases lead to a negative TEC, several researchers have used various methods to remove automated biases of the satellites and the receiver from GPS measurements. In general, the goal for all studies is to obtain an accurate estimate of TEC [3, 4].

Sardon et al. [5] assumed that DCB values for GPS satellites or receivers are constant over a period of one day or one month. Schaer and Steigenberger [6] went to the same proposition in estimate of DCB. Yan et al. [7] used the least square method to estimate the DCB of the GPS, while Arikan et al. [8] used another way to minimize the standard deviation (i.e. the true value with the constraint condition). Ma and Maruyama [9] said that the least square method is a good way

to estimate the DCB of the GPS. Li et al. [10] argued that DCB had a significant effect on TEC estimates and should be taken into account. Kunitsyn et al. [11] have shown that, when analysing geostationary SBAS TEC data, consideration should be given to the need to take into account spatial gradients of electron density. It has also been reported that long-term TEC datasets obtained from geostationary SBAS may have systematic variations related to DCB.

On the other hand, a number of studies have indicated the importance of correcting the effect of DCB precisely when designing specific GSP applications [12, 13].

Ciraolo et al. [14] reported that ignore the influences of DCB lead to an error of about 30u TEC. In another respect, Sardon and Néstor [15] showed that there is always some difference that occurs once a satellite is in orbit, despite the satellite's calibration. Wilson et al. [16] employed different way through the Jet Propulsion Laboratory to estimate and monitor GPS satellite DCB. Hernández-Pajares et al. [17] used the Ionospheric Working Group to estimate the DCB satellite and to develop Global Ionospheric Maps (GIM) based on GPS data. Reported that IGS is providing differential P1 / C1 code biases that are processed on the basis of the ionosphere-free linear combination. During the local night time, multiple authors analyzed data from a single station and modeled the vertical TEC with a quadratic latitude and longitude function. In addition, Abid et al. [4] has expanded the technique of attaching thin sphere shells to GPS network data sets. Also, other studies used global ionospheric total electron content and considered DCB as daily constants [13, 15]. Abid et al. [18] introduced Kriging interpolation as a simple and straightforward approach to the IGS reprocessing and improvement of ionospheric maps computed by other agencies.

This paper presents a more detailed analysis and continuous use of GPS data over 12 months (from January 1, 2014 to December 2014) to study day-to-day variation and long-term variation of GPS instrumental bias. This method which to

estimate the SDCB is calculate for first time in Egypt. The technical origin of instrumental biases is not discussed, but is estimated as a user estimating GPS data.

2. GPS DATA

There is no doubt that an increase in the number of GPS stations leads to an increase in the number of observations and data and thus to a better estimation of bias tools through data consolidation. In general, it can be said that, depending on the characteristics of the type of monitoring, the DCB differs for the GPS satellites. This indicates that increasing the number of stations helps to obtain accurate geodesy and survey applications. Consequently, this study relied on the use of nine local reference stations for the Global Positioning System (EPGN). The DCB analysis process took place over Egypt and the study covered more than 12 months of continuous data (i.e. from January to December 2014). The data sample rate is 1s Figure 1 shows the map featuring the nine GPS stations, while Table 1 shows the Cartesian coordinates of the stations considered.

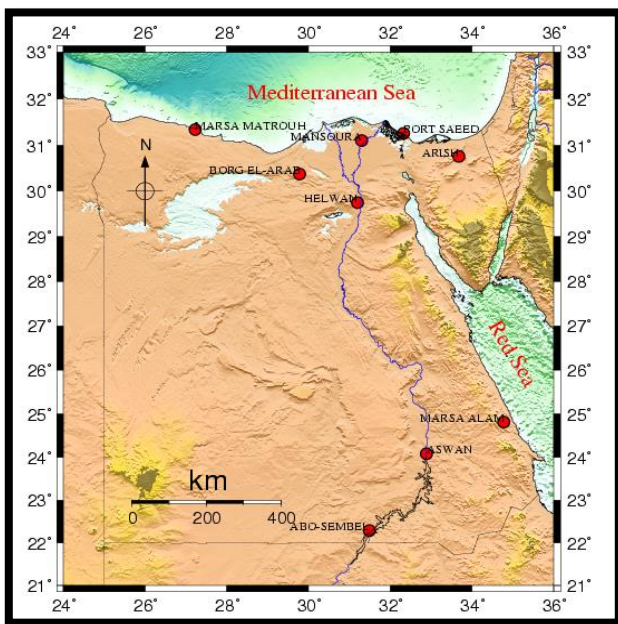


Figure 1. Location of the used GPS station

Table 1. Cartesian coordinates of the GPS sites

Station Id.	X (m)	Y (m)	Z (m)
PHLW	4728141.2348	2879662.6041	3157147.1275
SAID	4612664.2381	2917621.3718	3289234.9243
BORG	4765954.3185	2704546.1674	3252949.1622
ARSH	4551743.5738	3026108.3528	3276117.4525
ASWN	4899061.5611	3163086.8817	2575414.1543
ABSM	5024945.1535	3084578.9769	2424694.7180
ALAM	4742516.3847	3305688.9798	2685814.2467
MNSR	4671006.2282	2845893.5711	3269812.0787
MTRH	4847946.8930	2494773.3017	298721.2242

Herein, the following can be explained:

- The estimate of DCB is once a day (Daily variation of the DCB results taken into account).
- The Bernese V.5 is employed to estimate the satellite DCB values as well, determined it as daily value.
- Daily averages are found by calculating the total

average of the daily DCB satellite over a period of one day.

- The original Standard Product 3 format (Sp3) precise ephemeris orbits is employed to estimate the position of the satellite Details of these steps can be found in (ref).

3. DATA ANALYSIS

For this study used a collected data from a specific part of EPGN. In this part of EPGN, dual-frequency GPS receivers were used. The network covers an area of approximately 947km by 484km in longitude and latitude. Two different types of Trimble receivers, namely, Trimble 5700 and Trimble NETR5, were used to collect the required data. The records position was collected over one year; every month was represented by three different days, thereby resulting in 36 days of data per year. The original data were in receiver independent exchange format with one second sampling rate. An elevation cut-off angle of 10° was used for the collected data. The (SP3) and ionospheric models were imported from IGS.

4. DCB ESTIMATION

One of the advantages of the method used here is relying on data for a full year and using a reliable program to analyze and calculate the obtained values. Neglecting multipath and noise, a single pseudorange observation can be characterized:

$$P = \rho + c \delta^{rcv} - c \delta^{sat} + T + I + B \quad (1)$$

where:

Sum of a geometric range is (δ)

Satellite and receiver clock offsets (δt)

Tropospheric and ionospheric range delays (T, I)

Additive bias (B)

For the same satellite at frequencies f_{S1} and f_{S2} (Through tracking two distinct signals S_1 and S_2):

$$P_{S1} - P_{S2} = (I_{S1} - I_{S2}) + (B_{S1} + B_{S2}) \\ = 40.31 \text{ m}^3 \text{ s}^2 \cdot \left\{ \frac{1}{f_{S1}^2} - \frac{1}{f_{S2}^2} \right\} \cdot \text{STEC} + \text{DCB}_{S1-S2} \quad (2)$$

Then, differential code bias:

$$\text{DCB}_{S1-S2} = B_{S1} + B_{S2} \quad (3)$$

Furthermore, ionospheric delays may be added to the Slant Total Electron Content (STEC) if higher-order contributions are rejected. The orange pseudo difference explicitly provides the corresponding DCB for noise- and Multipath-free observations when two signals (or signals) are considered at a frequency. This enables, inter alia, the determination of GPS L1 and L2 frequency C / AP(Y) and L2C-P(Y) biases.

The combination of vertical TEC (VTEC) and the mapping feature m (E, elevation-dependent) are commonly referred to as the slant TEC for further processing.

$$\text{STEC} = \text{VTEC} \cdot m(E) \quad (4)$$

To simplify the status and according to the Figure 2.

$$m(E) = \frac{1}{\sin(E')} = \frac{1}{\sqrt{1 - \cos^2(E')}} \quad (5)$$

Then, the mapping feature is calculated through E' elevation at the IPP (i.e. ionospheric pierce point). The pierce point elevation is obtained from the Earth-observer-IPP triangle as regards the satellite seen from the given position on elevation E.

$$\cos(E') = \frac{R_{\oplus}}{R_{\oplus} + h} \cos(E) \quad (6)$$

For all contributing sites and all observed satellites, the combined satellite-plus-receiver DCBs are calculated. The use of (2)-(5) may be extracted from the arithmetic mean by a combined satellite-plus-receiver DCB.

$$DCB_{S1-S2} = \frac{1}{n} \sum_{i=1}^n [(P_{S1} - P_{S2}) - \Delta I]_i \quad (7)$$

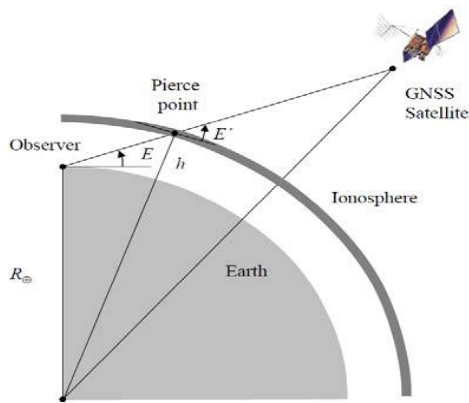


Figure 2. Single-layer ionosphere model

5. RESULTS AND STATISTICAL ANALYSIS

As mentioned earlier, in the four seasons in still geomagnetic conditions, the data employed for the performance analysis were chosen from those days. Accordingly, predicted DCB results from local station data used from IGS stations can be checked and validated. The findings suggest very strong consensus among the Bernese V 5.0 estimates used here by SDCBs and the Internet calculated IGS values with differences between them at the 3% level.

5.1 GPS satellite instrumental biases

For the 36 days studied, the derived SDCB at GPS satellites are shown in Figures 3-10. The daily changes in the SDCB depend on how well the VTEC Space distributions are equipped with the model. Picked here are a selection of Egyptian stations with distances between 94 km (MNSR – SAID) and 1069 km (MTRH – ABSM). During one year, a daily SDCB value, as well as a mean, was calculated for 3 days in each month. Furthermore, the cumulative DCB variations (difference between max. value and min. value) and the RMS value were determined for each satellite for the three-day duration.

For all PRN under consideration, the findings reflected the daily variation range and RMS of SDCB and it gives an indicator that the SDCB variation is very closed to each other. In this way, the test shows that it is closely related to the fitness

of the ionospheric model with the actual space distributions in the VTEC that calculated SDCB variations are present.

Although similar to one another, the day-to-day variation in SDCB is different at PRN. Between the day 1 and the day 36, it is about -13.463 at PRN 6 and 11.315 at PRN 22 is generally smaller in the summer and the winter at PRN 1 range from -11.18 to -9.783 and in the spring and the autumn at PRN range from -13.463 to -9.553, and is larger in the summer at PRN 20 range from 10.581 to 9.477 at PRN 19 and the autumn at PRN 31 range from 11.293 to 10.781 at PRN 32 the SDCB in the winter is a little larger than that in the summer. Generally, these outcomes are in accordance with the observations of the IGS SDCB. Table 2 shows the minimum and maximum value for SDCB.

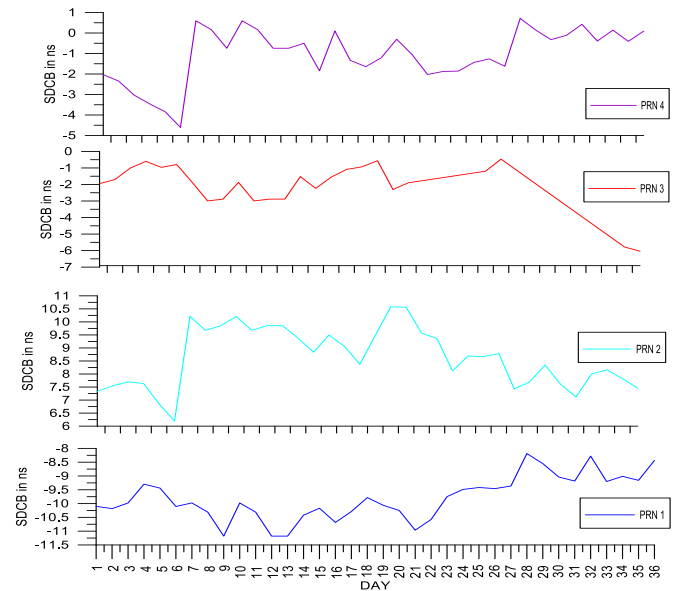


Figure 3. Satellite differential code bias estimates for PRN 1,2,3,4 from nine local stations

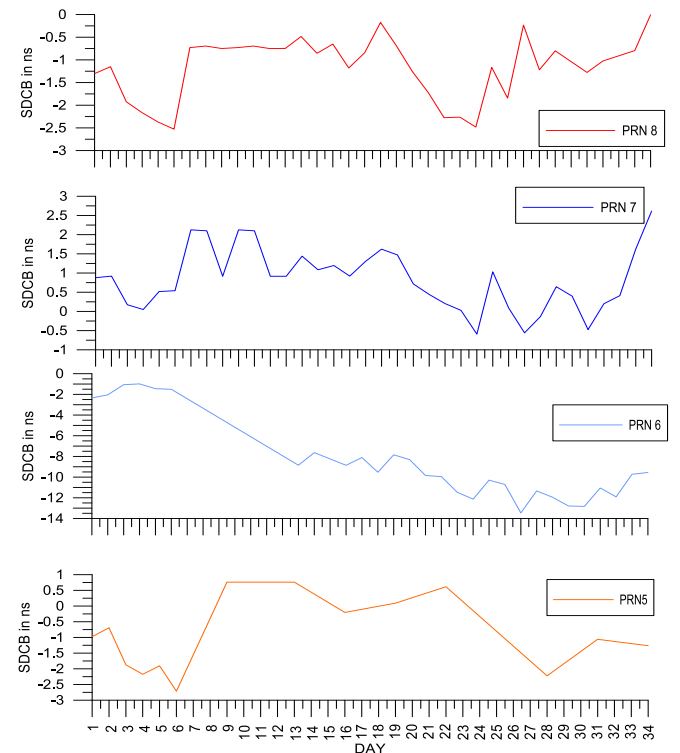


Figure 4. Satellite differential code bias estimates for PRN 5,6,7,8 from nine local stations

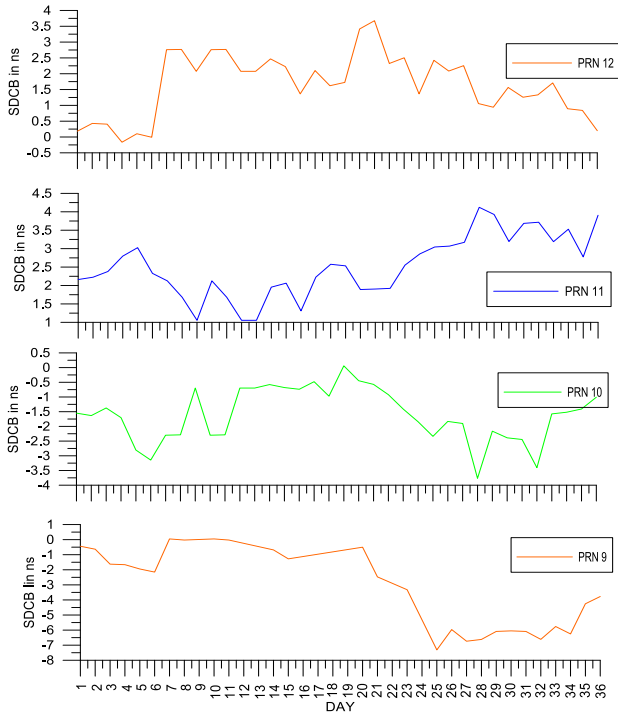


Figure 5. Satellite differential code bias estimates for PRN 9,10,11,12 from nine local stations

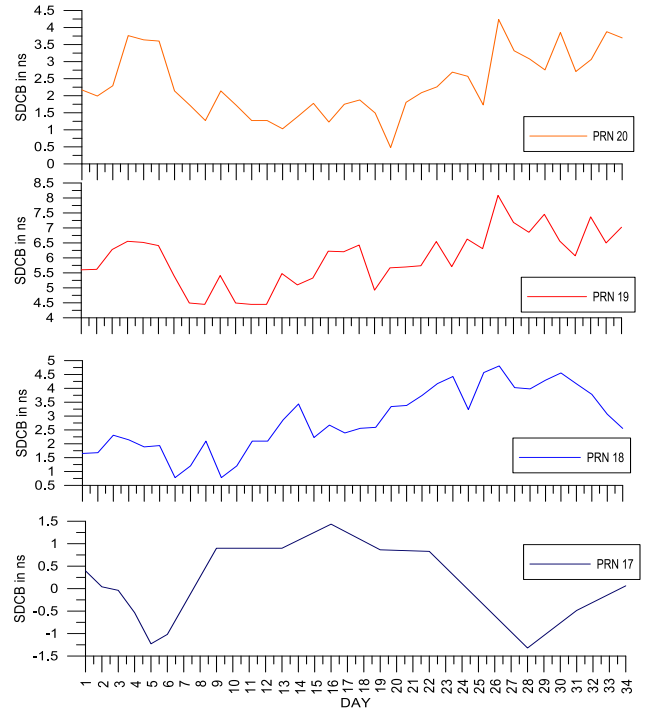


Figure 7. Satellite differential code bias estimates for PRN 17,18,19,20 from nine local stations

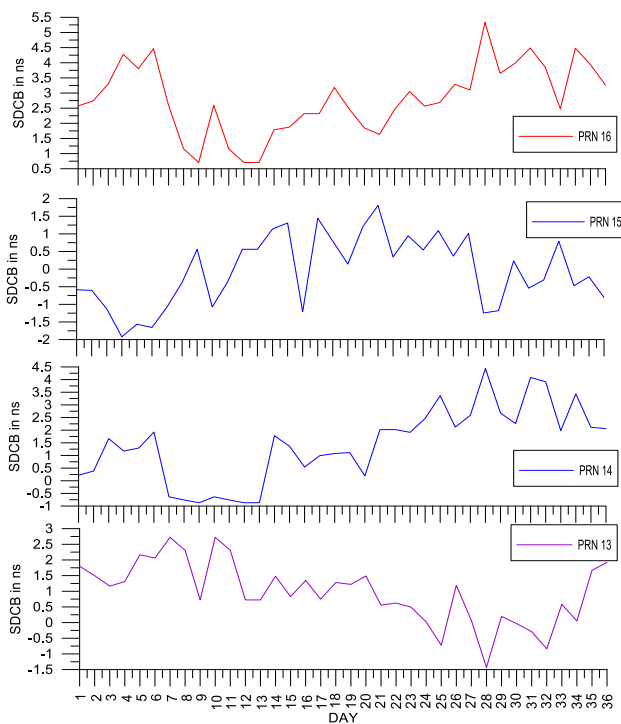


Figure 6. Satellite differential code bias estimates for PRN 13,14,15,16 from nine local stations

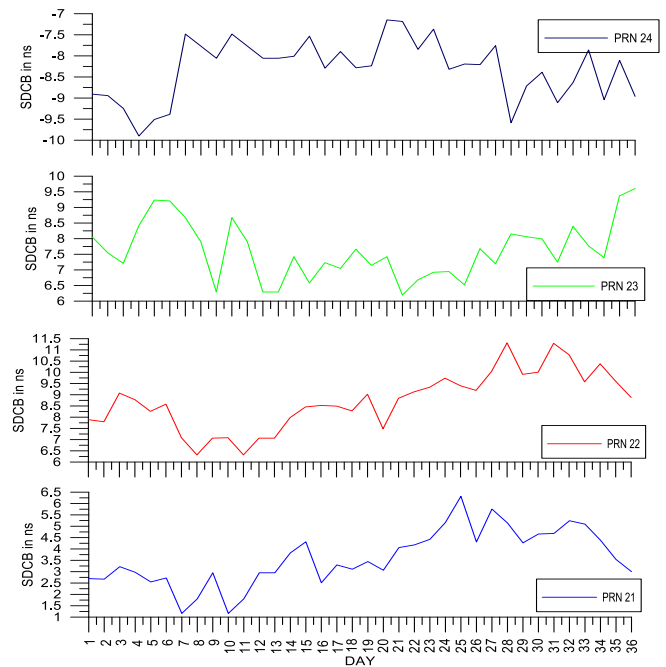


Figure 8. Satellite differential code bias estimates for PRN 21,22,23,24 from nine local stations

Table 2. The minimum and maximum value for SDCB

Figure	SDCB (ns)	
	Min.	Max.
1	-11.18 PRN1	10.58 PRN2
2	-13.46 PRN6	2.61 PRN7
3	-7.31 PRN9	4.12 PRN11
4	-1.92 PRN15	5.33 PRN16
5	1.32 PRN17	8.09 PRN19
6	-7.31 PRN9	4.12 PRN11
7	-9.44 PRN25	3.56 PRN28
8	-10.47 PRN30	8.23 PRN31

The RMS (in nanoseconds) of the GPS satellite instrumental biases relative to the mean. This RMS is smaller than 0.075 ns for all satellites, being the maximum for satellite PRN04. For some satellites, that RMS is even smaller than 0.060 ns: PRN 1, 6, 7, 8 and 9. For those satellites, there are neither abnormal values nor significant variations in their biases. The mean RMS of all satellites is 0.063 ns.

The SDCBs estimates for the 32 satellites in this area can be classified into various groups, provided that the maximum weather temperature variations occur in four seasons. The root mean squares (RMS) of instrumental biases for satellite are range from 0.012-o.014 ns.

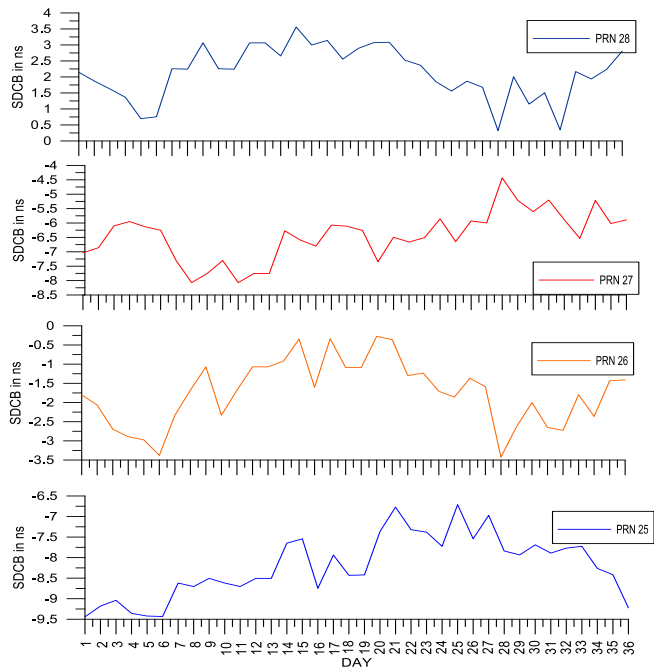


Figure 9. Satellite differential code bias estimates for PRN 25,26,27,28 from nine local stations

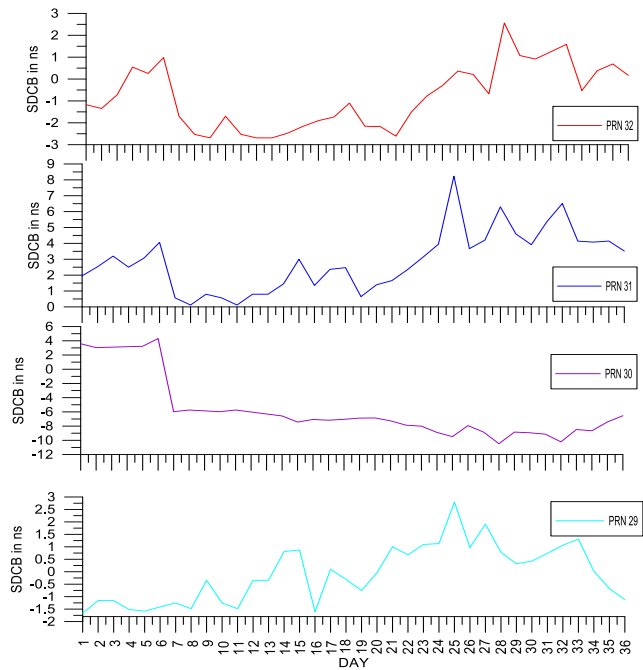


Figure 10. Satellite differential code bias estimates for PRN 29,30,31,32 from nine local stations

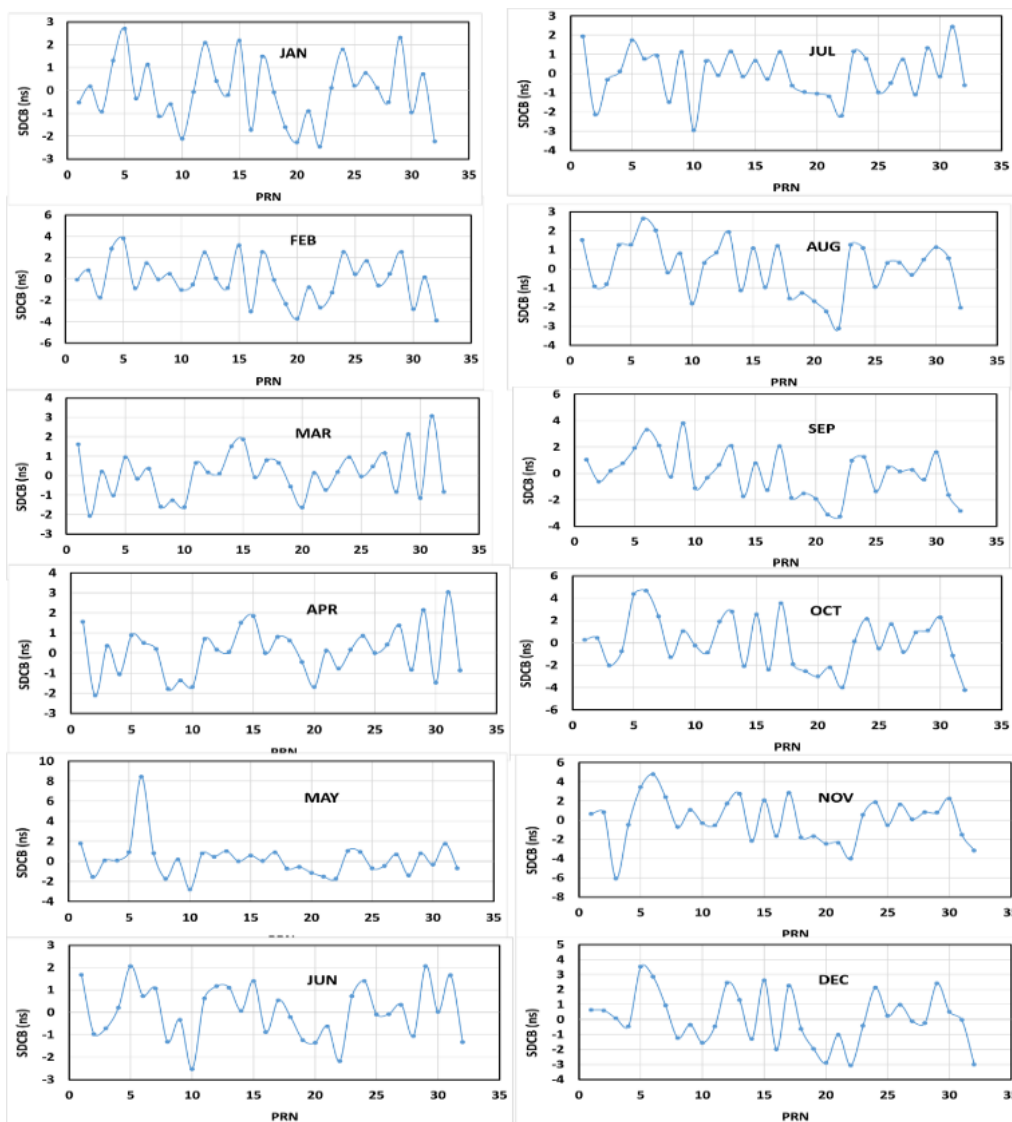


Figure 11. The diff. SDCB estimated and IGS value for one year

5.2 Monthly variation between satellite DCB estimates and IGS value

For the 12 month studied in 2014, the derived SDCB at GPS satellites are shown in Figure 11. Since Bernese V.5 selects various reference satellites on different days, there is an average variance between the different satellite DCB estimates and this disturbance must be eliminated before validation takes place.

The overall bias was first eliminated from the regular DCB estimates, taking CODE estimates as normal. Secondly, the average of all daily DCB forecasts during 36 days of data collection was determined for each satellite monthly.

Then, monthly DCB estimates by Bernese and CODE obtained and presented in Figure 11 on the basis of these two steps. For Winter the variation between the estimated values and IGS values range from -3.88 to 3.81 ns, in Spring the variation range between estimated and IGS from -2.8 to 3.04 ns, while Summer the result of estimated and IGS vary from -3.26 to 3.81 ns, in Autumn the differ between the two values vary from -3.98 to 3.43 ns. All this doing to find if is there a difference in results between seasons or not.

6. SUMMARY AND CONCLUSIONS

The data used are collected from nine globally distributed tracking stations located in the Egypt region in Africa, which cover various levels of solar activity and various geographical locations. In this paper, Bernese V.5 is employed to determine the GPS satellites biases where this way is applied to the GPS chain observations during four seasons of 2014 (totally 36 days). Also, the findings show that the DEB of GPS satellites are rather stable where the RMS where the RMS ranges from 0.197 ns to 1.280 ns during the test period, i.e. 0.09 ns. Additionally, the satellite biases are also related to CODE biases. From the results, it can be clearly inferred that the Bernese SDCB estimates are close in quality to those reported by CODE.

The results showed the preference of the approach used in the study, which is the Bern approach, as this approach does not require a large group of ground deviations compared to the adopted approach, which requires a large amount of data and a large number of stations. In another way, the satellite DCB resolution obtained through the IGS approach reached the same level as for the current methods (about 0.23-0.27 ns).

The outcomes uncover clear diurnal day-to-day and seasonal variations. The study obtained precise estimation of the biases of the 32 GPS satellites available during the observation campaigns and of the receivers at the 9 stations. The satellite biases relative to the mean estimate for four different epochs spanning 1 year show a variation smaller than 2 ns. When looking at the daily variance in global positioning system (GPS) biases relative to the mean, it appears evident that the variance in the estimated satellite biases between successive days is less than 0.2 ns in more than 80% of cases. The assessment analysis has shown that DCB of GPS satellites, the maximum difference was 2nd, and this means that the two SDCB estimates are more consistent with each other.

REFERENCES

[1] Coco, D.S., Coker, C., Dahlke, S.R., Clynych, J.R. (1991).

- Variability of GPS satellite differential group delay biases. *IEEE Transactions on Aerospace and Electronic Systems*, 27(6): 931-938. <https://doi.org/10.1109/7.104264>
- [2] Leandro, R.F., Langley, R.B., Santos, M.C. (2007). Estimation of P2-C2 biases by means of precise point positioning. In *Proceedings of the ION 63rd Annual Meeting*, pp. 23-25.
- [3] Lanyi, G.E., Roth, T. (1988). A comparison of mapped and measured total ionospheric electron content using global positioning system and beacon satellite observations. *Radio Science*, 23(4): 483-492. <https://doi.org/10.1029/RS023i004p00483>
- [4] Abid, M.A., Mousa, A., Rabah, M., El mewafi, M., Awad, A. (2016). Temporal and spatial variation of differential code biases: A case study of regional network in Egypt. *Alexandria Engineering Journal*, 55(2): 1507-1514. <https://doi.org/10.1016/j.aej.2016.03.004>
- [5] Sardon, E., Rius, A., Zarraoa, N. (1994). Estimation of the transmitter and receiver differential biases and the ionospheric total electron content from Global Positioning System observations. *Radio Science*, 29(3): 577-586. <https://doi.org/10.1029/94RS00449>
- [6] Schaer, S., Steigenberger, P. (2006). Determination and use of GPS differential code bias values. In *IGS workshop*, pp. 8-11.
- [7] Yan, J.G., Li, F., Ping, J.S., Dohm, J.M., Harada, Y., Zhong, Z. (2012). A simulation of Martian gravity field recovery by using a near equatorial orbiter. *Advances in Space Research*, 49(5): 1019-1027. <https://doi.org/10.1016/j.asr.2011.12.006>
- [8] Arikan, F.E.Z.A., Nayir, H., Sezen, U.M.U.T., Arikan, O. (2008). Estimation of single station interfrequency receiver bias using GPS-TEC. *Radio Science*, 43(4): 1-13. <https://doi.org/10.1029/2007RS003785>
- [9] Ma, G., Maruyama, T. (2003). Derivation of TEC and estimation of instrumental biases from GEONET in Japan. *Annales Geophysicae*, 21(10): 2083-2093. <https://doi.org/10.5194/angeo-21-2083-2003>
- [10] Li, Z.S., Yuan, Y.B., Li, H., Ou, J.K., Huo, X.L. (2012). Two-step method for the determination of the differential code biases of COMPASS satellites. *Journal of Geodesy*, 86(11): 1059-1076. <https://doi.org/10.1007/s00190-012-0565-4>
- [11] Kunitsyn, V., Kurbatov, G., Yasyukevich, Y., Padokhin, A. (2014). Investigation of SBAS L1/L5 signals and their application to the ionospheric TEC studies. *IEEE Geoscience and Remote Sensing Letters*, 12(3): 547-551. <https://doi.org/10.1109/LGRS.2014.2350037>
- [12] Conte, J.F., Azpilicueta, F., Brunini, C. (2011). Accuracy assessment of the GPS-TEC calibration constants by means of a simulation technique. *Journal of Geodesy*, 85(10): 707. <https://doi.org/10.1007/s00190-011-0477-8>
- [13] Komjathy, A., Sparks, L., Wilson, B.D., Mannucci, A.J. (2005). Automated daily processing of more than 1000 ground-based GPS receivers for studying intense ionospheric storms. *Radio Science*, 40(6): 1-11. <https://doi.org/10.1029/2005RS003279>
- [14] Ciraolo, L., Azpilicueta, F., Brunini, C., Meza, A., Radicella, S.M. (2007). Calibration errors on experimental slant total electron content (TEC) determined with GPS. *Journal of Geodesy*, 81(2): 111-120. <https://doi.org/10.1007/s00190-006-0093-1>
- [15] Sardón, E., Zarraoa, N. (1997). Estimation of total

- electron content using GPS data: How stable are the differential satellite and receiver instrumental biases? *Radio Science*, 32(5): 1899-1910. <https://doi.org/10.1029/97RS01457>
- [16] Wilson, B., Yinger, C., Feess, W., Shank, C. (1999). New and improved-the broadcast interfrequency biases. *GPS World*, 10(9): 56-66.
- [17] Hernández-Pajares, M., Juan, J.M., Sanz, J. (1999). New approaches in global ionospheric determination using ground GPS data. *Journal of Atmospheric and Solar-Terrestrial Physics*, 61(16): 1237-1247. [https://doi.org/10.1016/S1364-6826\(99\)00054-1](https://doi.org/10.1016/S1364-6826(99)00054-1)
- [18] Abid, M.A., Husein, H.N., Hamed, N.H. (2020). Analysis of error in geodetic networks using different observation methods. *IOP Conference Series: Materials Science and Engineering*, Istanbul, Turkey. <https://doi.org/10.1088/1757-899X/737/1/012234>